A STUDY ON EROSION AND CORROSION BEHAVIOR OF Cr_3C_2-NiCr CERMET COATINGS

Ha Pham Thi[1, *], Tuan Nguyen Van[1], Quy Le Thu[2], Tuan Anh Nguyen[1], Ly Pham Thi[1], Cuong Ly Quoc[1], Thuy Dao Bich[1]

[1]*Institute for Tropical Technology, VAST,
18 Hoang Quoc Viet, Cau Giay, Ha Noi*

[2]*National Key Laboratory for Welding and Surface Treatment Technologies, NARIME,
4 Pham Van Dong, Cau Giay, Ha Noi*

[*]Email: *hapham205@gmail.com*

ABSTRACT

In this study, Cr_3C_2-NiCr cermet coating samples were prepared by atmospheric plasma spraying (APS) technique on 410 stainless steel substrate with different plasma spraying parameters, namely, the powder feed rate (10 and 30 g.min^{-1}) and the plasma current (500 and 600 A). The erosion-corrosion behaviour of the coatings was studied by electrochemical measurements, salt spray and erosion-corrosion tests. The electrochemical tests were performed in 3.5 wt.% NaCl solution. During the erosion-corrosion test, the samples were immersed in 3.5 wt.% NaCl solution containing 0.25 wt.% SiO_2 particles with a rotational speed of 950 rpm for 72 hours. The obtained results showed that the plasma sprayed coating sample at the plasma current of 600 A and the powder feed rate of 10 g/min has a best erosion-corrosion resistance. Red rust spots did not appear on surface of this coating after 120 hours of salt spray test. It was much slower than on the others (after only 24 hours salt spray test). The weight loss of this coating during the erosion-corrosion test was lower than the remaining samples. These results are consistent with the results of electrochemical tests.

Keywords: plasma spraying, cermet coating, erosion-corrosion, Cr_3C_2-NiCr.

1. INTRODUCTION

Erosion and corrosion are the common problems been faced by many industries such as aerospace, chemical, petroleum, automotive and energy power, which caused great economic losses [1]. An effective way to prevent the erosion - corrosion is to use thermal spray coatings. The coatings of Cr_3C_2–NiCr, WC-Co-Cr, Al_2O_3-TiO_2, etc. are extensively used in a wide variety of applications like gas turbines, boilers, aircrafts, etc. [2].

At high temperatures where WC-based coatings are not suitable, meanwhile Cr_3C_2–NiCr coatings have been extensively used to minimize wear and corrosion [3]. In this case, NiCr alloy serves as a matrix that improves overall coating integrity and corrosion resistance, while Cr_3C_2

constituent serves as a hard phase that assures wear resistance. These coating properties together effectively combat solid particle erosion, high-temperature wear (abrasion, erosion, fretting and cavitation) up to 870 ^{o}C and hot corrosion [4].

Erosion and corrosion properties of Cr_3C_2–NiCr cermet coating have been previously studied [4-7, 8-9]. Guilemany *et al.* have studied the corrosion properties of these coatings in three corrosive media (3.4 % NaCl, 0.5 % H_2SO_4 and alkaline solutions) [6]. The authors indicated that the absence of pores and cracks play an important role in preserving the integrity of the coating–substrate system, as these defects are mainly used by the electrolyte to reach the steel substrate. The corrosive wear behavior of Cr_3C_2–NiCr coatings was studied in hydrochloric acid environment, through wet pin-on-disk wear experiments [7]. The results showed that the wet environment significantly increased the wear rate. The wear mechanism in the dry sliding was abrasive. This mechanism changes in the wet environments to the adhesive. An increase of the acid concentration and temperature considerably deteriorated the wear resistance of the coated samples.

Since the quality of the coating depends on a large number of parameters, the optimization of spraying parameters is important for obtaining high-quality coating [10]. In present work, Cr_3C_2-NiCr coatings were deposited on 410 stainless steel substrate by atmospheric plasma spraying technique with different plasma spraying parameters. The software Modde 5.0 was used for design of experiments in order to select the optimum technology mode for low porosity and high hardness of the coatings. The optimum chosen coating sample was then used for erosion-corrosion tests. The sprayed-coatings at center mode and recommended mode by PRAXAIR-TAFA also were selected for survey purposes to compare. The erosion-corrosion behaviour of the coatings was studied by using electrochemical measurements, salt spray and erosion-corrosion tests.

2. MATERIALS AND METHODS

2.1. Materials and preparation of samples

75Cr₃C₂-25NiCr (wt.%) powder with the chemical composition: $C \leq 0.2$ %, $Si \leq 0.5$ %, NiCr 24.5 % and Cr_3C_2 74.8 % and nominal size of 25–40 μm of Wisdom Consumables (Shanghai, China) has been used to spray on 410 stainless steel substrate ($50 \times 50 \times 5$ mm). Prior to the spraying, the surfaces of samples were degreased with acetone and then grit blasted with corundum to get a surface with a mean roughness of around 60 μm. Cr_3C_2-NiCr coatings were obtained using Tafa 3710-PRAXAIR (US) plasma spray equipment with flow rate of Ar gas of 70 L.min^{-1}, flow rate of H_2 gas of 3 L.min^{-1} and spraying distance of 100 mm. The powder feed rate and the plasma current parameters are shown in Table 1.

Table 1. Thermal spray parameter.

Sample labeling	Plasma current (A)	Powder feed rate, g.min^{-1}	Note
M1	600	10	Optimal mode
M2	500	30	Center mode
M3	500	10	Recommended mode by PRAXAIR-TAFA

The software Modde 5.0 was used for design of experiments for investigating the influence of the spraying parameter on the structure and properties of the coatings. This method minimized the number of experiments and offered a scientifically optimal mode. In this study, we selected 3 modes for comparative study. There are optimal mode (M1), center mode (M2), and recommended mode by PRAXAIR-TAFA (M3).

2.2. Analytical methods

The microstructure of powder and coatings was studied using a scanning electron microscope JEOL JMS-6490 (Japan). Electrochemical properties of the coatings in 3.5 wt.% NaCl solution at ambiance were investigated by potentiodynamic polarization measurement and electrochemical impedance spectroscopy (EIS) measurement using the VSP-300 multichannel potentiostat/galvanostat (Bio-Logic Science Instruments, France). The electrochemical tests were performed in a three-electrode cell using a platinum plate as counter electrode, a SCE as reference electrode and the coating sample as the working electrode. The polarization curves were obtained at a scan rate of 1 mV/s and a scan range of -500 mV to 500 mV/SCE around the open circuit potential (E_{ocp}) [9, 10]. The corrosion potential and the corrosion current density were obtained through the linear analysis of Tafel approximation. Electrochemical impedance spectroscopy (EIS) measurements were carried out at the open circuit potential (E_{ocp}) after 2 hours of immersion. The frequency range varied from 10^{-2} Hz to 10^5 Hz with 7 points per decade, potential amplitude $\Delta E = 5$ mV. The salt spray test was carried out according to ASTM B117 standard using Q-FOG Cyclic Corrosion Tester CCT 600 (USA) with 5 wt.% NaCl solution for 144 hours. The erosion corrosion resistance of the coatings was tested in a slurry flow of 3.5 wt.% NaCl solution containing 0.25 % SiO_2 solid grains (grain size 100-150 μm) with a rotational speed of 950 rpm for 72 hours [11, 12]. The mass loss during erosion corrosion test was monitored over time with analytical balance of 0.0001 g accuracy.

3. RESULTS AND DISCUSSION

3.1. Microstructure analysis

Figure 1. Structural morphology of 75Cr$_3$C$_2$-25NiCr powders (a) and cross-sectional structures of Cr$_3$C$_2$-NiCr coating (b).

The structural morphology of 75Cr$_3$C$_2$-25NiCr powders and cross-sectional structures of Cr$_3$C$_2$-NiCr coating are shown in Fig. 1a and 1b, respectively. According to Fig. 1a, the powder

particle size is in a range of 25–40 μm. The powder had a predominantly spherical morphology. Fig. 1b shows the coating thickness of about 300-350 μm. There exist many unmelted particles and pores in the coating.

3.2. Electrochemical measurement

Potentiodynamic polarization curves of the three coatings and 410 stainless steel substrate in 3.5 wt.% NaCl solution and the corrosion parameters determined from these curves are shown in Fig. 2 and Table 2. The results shows that, the corrosion potential of M1 sample (-0.63 V/SCE) was more negative than that of other two samples (-0.57 V/SCE) and stainless steel substrate (-0.3 V/SCE). Moreover, M1 sample had lowest corrosion current density. The value of corrosion current density corresponding to M1, M2 and M3 samples are 4.76, 10.18 and 8.46 μA.cm^{-2}, respectively. Therefore, M1 sample (600 A, 10 g.min^{-1}) showed the best performance among the coatings to protect the stainless steel substrate against corrosion in NaCl solution.

Table 2. The corrosion parameters of the coatings after 2 hours of immersion in 3.5 wt.% NaCl solution.

Sample	i$_{corr}$ (μA/cm^2)	E$_{corr}$ (V/SCE)
M1	4.76	-0.63
M2	10.18	-0.57
M3	8.46	-0,57
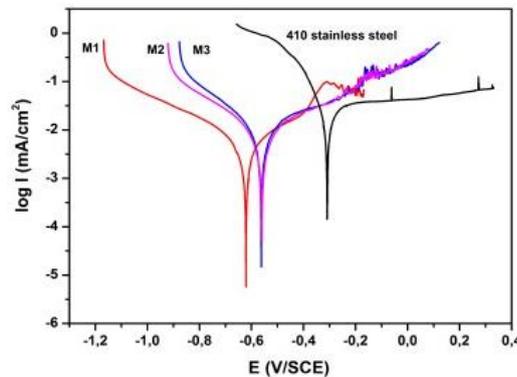
Figure 2. Polarization curves of Cr$_3$C$_2$-NiCr coatings and stainless steel substrate after 2 hours of immersion in 3.5 wt.% NaCl solution.

Figure 3 and Fig. 4 show Nyquist plots and Bode plots of Cr$_3$C$_2$-NiCr coatings after 2 hours of immersion in 3.5 wt.% NaCl solution. In Bode plots, the magnitude of the impedance |Z| are plotted respectively as a function of frequency (f). Impedance at the high frequency region represents the performance of the coating in corrosion solution. While at the low frequency, it is related to the corrosion at the substrate/solution interface [13]. The obtained results show that, at the low frequency, M1 sample exhibits the impedance |Z| greater than that of M2 and M3 samples (3286.70, 1099.82, 1753.07 Ω, respectively). In Nyquist plots, two semicircles are observed for all spectra of the samples, thus the equivalent circuit [R$_s$(R$_1$Q$_1$)(R$_2$Q$_2$)] accurately fit the experimental data. The parameters were obtained by fitting the experimental data using EC-lab V11.02 software. R$_s$ is the solution resistance. The constant phase element Q substitutes

the capacitance C for heterogeneous and rough surfaces. The (R_1Q_1) is associated to the solution resistance of the electrolyte into the pores (R_1) and the capacitance of the layer that is the coating (Q_1). The R_1, related to the resistance of the solution into the pores of the coating, is higher for M1 sample than M2 and M3 samples (367, 86, 109 Ω, respectively). The (R_2Q_2) was linked to the charge transfer resistance related to the substrate oxidation (R_2) and the capacitance of the electrical double layer (Q_2). The R_2 value for M1 sample is higher than M2 and M3 samples (3130, 1113, 1736 Ω, respectively). Combined with polarization curves results, it can be assumed that M1 sample was more corrosion resistant than the remaining samples.
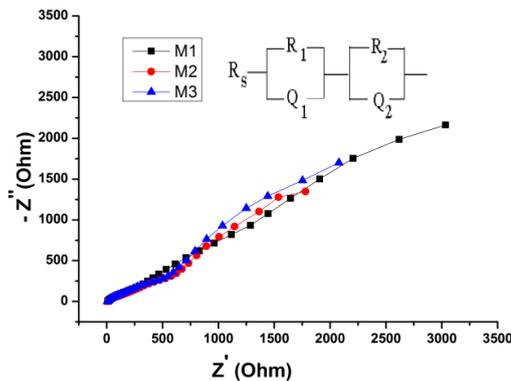
Figure 3. Nyquist plots of Cr_3C_2-NiCr coatings after 2 hours of immersion in 3.5 wt.% NaCl solution.
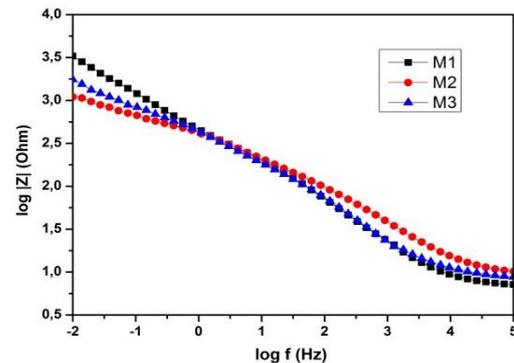
Figure 4. Bode plots of Cr_3C_2-NiCr coatings after 2 hours of immersion in 3.5 wt.% NaCl solution.

3.3. Salt spray resistance

After salt spray test for 144 hours with 5 % NaCl solution, the results of surface observation of the Cr_3C_2-NiCr coatings are shown in Fig. 5. After only 24 hours of test, the red rust spots began to appear on the surface of M2 and M3 samples and then spreaded with time over the test period. Meanwhile, after 120 hours of test, the red rust spots began to appear on the surface of M1 sample. However after 144 hours test, the rust spots did not spread. This rust spots may be the defect parts of the coating and it is not represent to the coating. Thus in conclusion, red rust spots did not appear on surface of M1 coating sample after 120 hours of salt spray test. This shows that salt spray resistance of M1 sample is higher than that of M2 and M3 samples. These results are consistent with the results of the electrochemical test.

As a result, the plasma current and powder feed rate have significantly affected corrosion resistance of the coatings. The M1 coating (600 A, 10 g.min^{-1}) has higher corrosion resistance than M2 (500 A, 30 g.min^{-1}) and M3 (500 A, 10 g.min^{-1}) coatings. The plasma current and powder feed rate are closely related to the melting ability of powder. In condition of high powder feed rate with low plasma current, the powder did not receive enough energy to completely melt thus affecting the structure of coating. The sprayed coating has high porosity. Thus the corrosion solution is easily absorbed deep into the coating. Decreasing powder feed rate and increasing plasma current causes more particles to be melted during the spray process, though stresses would be lessen and finally general quality of the coating increases [10]. However, if the plasma current is too large, the steel substrate will be thermally deformed and the sprayed coating has many cracks.

Time	M1	M2	M3
Initial			
After 2h			
After 8h			
After 24h			
After 48h			
After 72h			
After 96h			
After 120h			
After 144h			

Figure 5. Surface change of Cr₃C₂-NiCr coating samples during the salt spray test.
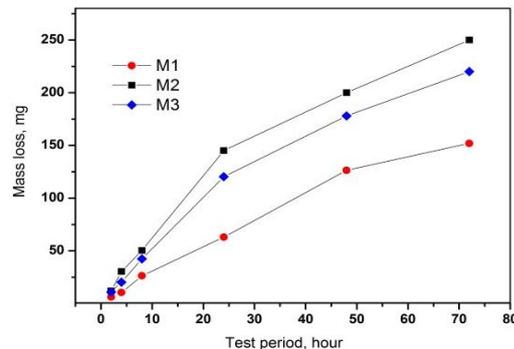
3.4. Erosion corrosion resistance

Figure 6. Erosion corrosion resistance of coatings.

Figure 6 presents the results of the erosion corrosion test for 72 hours. The result shows that, the mass loss of M2 and M3 samples are higher than that of M1 sample at all times of testing. After 72 hours of test, the mass loss of M1, M2 and M3 samples are 130.25, 280.20 and 212.40 mg, respectively. This is explained by increasing the plasma current, more energy was provided to the plasma beam. As a result, more particles melted and more coherent bonding between the splats in the coating hence the hardness of coating increased [10]. Thus, the plasma sprayed coating sample at the plasma current of 600 A and the powder feed rate of 10 g.min^{-1} (M1 sample) has a best erosion corrosion resistance.

4. CONCLUSIONS

Cr_3C_2-NiCr cermet coatings were prepared by atmospheri*c* plasma spraying (APS) technique on 410 stainless steel substrate with different plasma spraying parameters. The parameters setting such as plasma current and powder flow rate have provided evidence to directly influence the properties and performance of Cr_3C_2-NiCr coating.

The obtained results indicate that the plasma sprayed coating sample at the high plasma current of 600 A and the low powder feed rate of 10 g.min^{-1} has a best erosion corrosion resistance. This coating had lowest corrosion current density in electrochemical test. Red rust spots did not appear on surface of this coating until 120 hours of salt spray test. It was much slower than on the other coating samples (after only 24 hours salt spray test). The weight loss of this coating during the erosion corrosion test was the lowest in comparison with other coating samples.

REFERENCES

1. Zhang H., Dong X., Chen S. - Solid particle erosion-wear behaviour of Cr_3C_2–NiCr coating on Ni-based superalloy, Adv. Mec. Eng. **9** (3) (2017) 1–9.

2. Mehta J., Mittal V. K., Gupta P. - Role of Thermal Spray Coatings on Wear, Erosion and Corrosion Behavior: A Review, App. Surf. Sci. **20** (4) (2017) 445-452.

3. Matthews S., Hyland M., James B. - Microhardness variation in relation to carbide development in heat treated Cr$_3$C$_2$–NiCr thermal spray coatings, Acta Mater. **51** (2003) 4267–4277.

4. Zavareh M. A., Sarhan A. A. D. M., Zavareh P. A., Razak B. B. A., Basirun W. J., Ismail M. B. C. - Development and protection evaluation of two new, advanced ceramic composite thermal spray coatings, Al$_2$O$_3$–40TiO$_2$ and Cr$_3$C$_2$–20NiCr on carbon steel petroleum oil piping, Ceram. Int. **42** (2016) 5203–5210.

5. Zavareh M. A., Sarhan A. A. M., Razak B. B. A., Basirun W. J. - The tribological and electrochemical behavior of HVOF sprayed Cr$_3$C$_2$–NiCr ceramic coating on carbon steel, Ceram. Int. **41** (2015) 5387-5396.

6. Guilemany J. M., Espallargas N., Suegama P.H., Benedetti A. V., Comparative study of Cr$_3$C$_2$–NiCr coatings obtained by HVOF and hard chromium coatings, Corrosion Science **48** (2006) 2998-3013.

7. Yaghtin A. H., Salahinejad E., Khosravifard A., Araghi A., Akhbarizadeh A. - Corrosive wear behavior of chromium carbide coatings deposited by air plasma spraying, Ceram. Int. **41** (2015) 7916–7920.

8. Suarez M., Bellayer S., Traisnel M., Gonzalez W., Chicot D., Lesage J., Puchi Cabrera E. S., Staia M. H. - Corrosion behavior of Cr$_3$C$_2$–NiCr vacuum plasma sprayed coatings, Surf. Coat. Tech. **202** (2008) 4566-4571.

9. Guilemay J. M., Fernández J., Delgado J. - Electrochemical measurement and characterization of a thermal sprayed HVOF Cr$_3$C$_2$–NiCr coating in a corrosive environment, Proc. 2nd United Thermal Spray Conference [UTSC'99], DVS, Dusseldorf, Germany, p. 474, March 17–19, 1999.

10. Djendel M., Allaoui O., Bouzid A. - Effect of Air Plasma Spraying Parameters on the Quality of Coating, International Journal of Computational and Experimental Science and Engineering **2** (2) (2016) 1-5.

11. Abbade N. P., Crnkovic S. J. - Sand water slurry erosion of API. 5L X65 pipe steel as quenched from intercrid temperature, Tribology International **33** (2000) 811-816.

12. Fang Q., Xu H., Sidky P. S., Hocking M. G. - Erosion of ceramic materials by sand/water slurry jet, Wear **224** (1999) 183-193.

13. Shao F., Yang K., Zhao H., Liu C., Wang L., Tao S. - Effects of inorganic sealant and brief heat treatment on corrosion behavior of plasma sprayed Cr$_2$O$_3$-Al$_2$O$_3$ composite ceramic coatings, Surf. Coat. Tech. **276** (2015) 8-15.